SUPPORTING INFORMATION

Reconstruction of the carbon sp^2 network in graphene oxide by low-temperature reaction with CO

Angeles Pulido,[†] Patricia Concepción,[†] Mercedes Boronat,[†] Cristina Botas,[‡] Patricia Alvarez,[‡] Rosa Menendez,[‡] Avelino Corma[*,†]

[†]Instituto de Tecnología Química (UPV-CSIC), Universidad Politécnica de Valencia-Consejo Superior de Investigaciones Científicas, Av. de los Naranjos s/n, E-46022 Valencia, Spain.

[‡]Instituto Nacional del Carbón, CSIC, Apartado 73, E-33080 Oviedo, Spain

Supporting Information. Description of graphite, graphene oxide and partially reduced graphene oxide characterization procedures, as well as computational details.

Contents

S1. Characterization of parent graphite

      Optical microscopy

      XRD

S2. Characterization of graphene oxide and partially reduced graphene oxide

      AFM microscopy
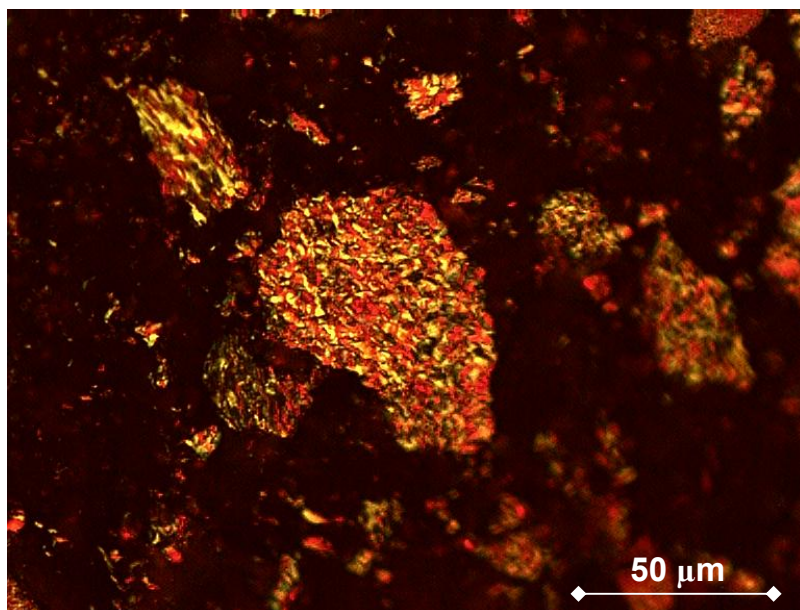
      TEM microscopy

      Raman spectroscopy

      XPS spectroscopy

      FTIR spectroscopy

S3. Computational details

References

S. 1. Characterization of parent graphite

Figure S1 . Optical micrograph of the parent graphite showing an optical texture of mosaics (1.5-5 μm). Samples were first embedded in an epoxy resin, then polished and finally examined using polarized light. The microscope was equipped with an adjusted ocular (10X), an oil-immersion objective (20X, 50X and 100X) and a 1-wave retarder plate.

X-ray Diffraction (XRD) was performed using a Bruker D8 Advance diffractometer. The radiation frequency used was the Kα1 line from Cu (1.5406 Å), with a power supply of 40 kV and 40 mA. The crystallite size along the c-axis (Lc) was obtained from the (002) reflection of the XRD patterns, which were recorded at steps of 0.01º and at intervals of 6 s per step, using the Scherrer equation. The crystallite size along the a-axis (La) was calculated from the (100) Bragg peak.

S2. Characterization of graphene oxide and partially reduced graphene oxide

For all of the characterization techniques employed a drop of a highly diluted water solution of the graphenic samples was deposited onto a carbon grid (TEM), a mica

substrate (AFM), a glass substrate (Raman), a Molybdenum sample holder (XPS) and a Germanium disc (FTIR).

AFM microscopy

The height and area of the sheets were measured using more than 75 different sheets for each sample. In order to obtain a more reliable statistical result for the sheet heights, histograms were constructed by measuring the distance between the first peak, corresponding to the substrate, and the second peak.
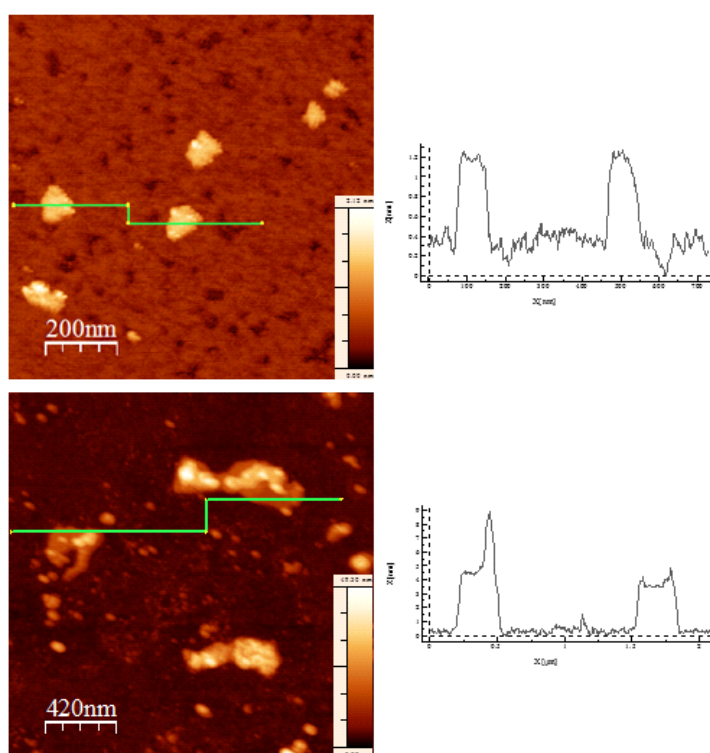

Figure S2. AFM Images of GO (top) and RGO (bottom) sheets. The horizontal lines indicate the sections corresponding to the traces shown on the right. The samples were imaged under exactly the same conditions ($\approx$ 20 ºC temperature and $\approx$ 30 % relative humidity). The GO and RGO sheets were imaged using a Cervantes atomic force microscope from Nanotec Electronica™ (www.nanotec.es) operating under ambient conditions. Microcantilevers with nominal spring constants of k = 40 N/m and a resonance frequency of f = 300 kHz were used to image the GO sheets. WSxM software[1] was employed to control the atomic force microscope in order to process the data from the acquired images.
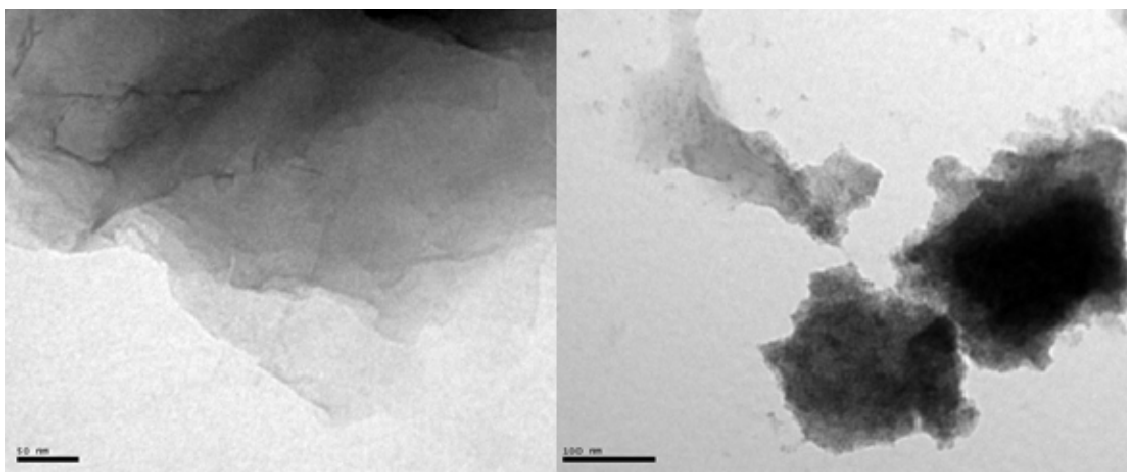
Figure S3. TEM images showing individual platelets extending from a particle composed of agglomerated sheets of GO (left) and RGO (right). Transmission electron microscopy (TEM) observations were performed on a JEOL 2000 EX-II instrument operating at 160 kV.

Raman spectroscopy
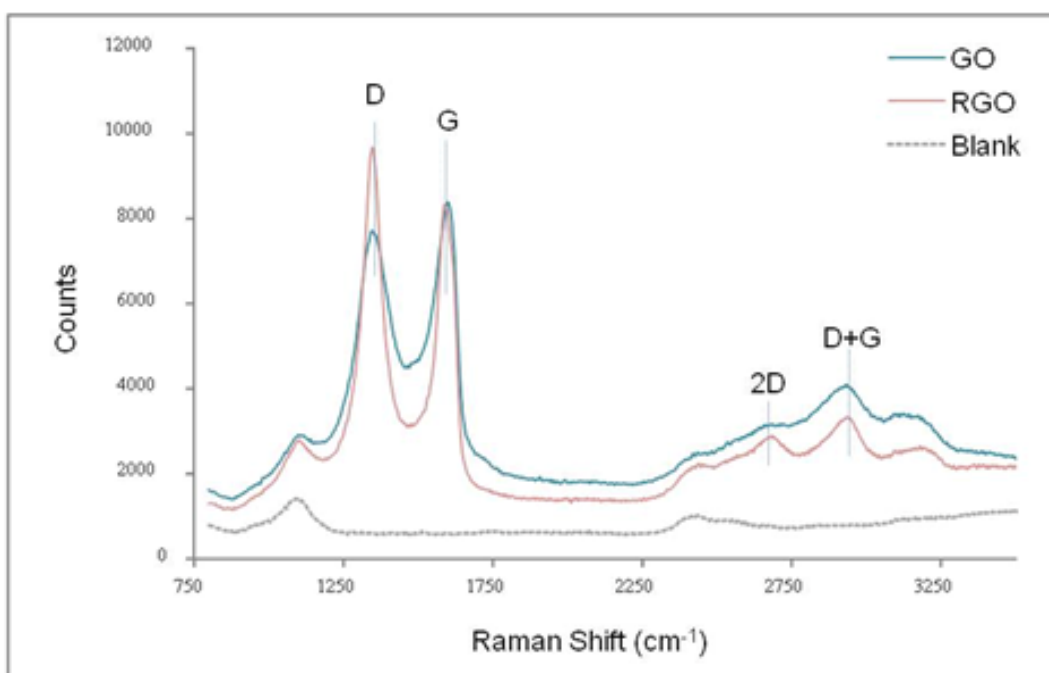
Figure S4. Raman spectra of the GO and RGO samples. Spectra were recorded at ambient temperature by means of a 514 nm laser excitation on a Renishaw Raman Spectrometer ("in via") equipped with a CCD detector. The laser power on the sample was set at 25 mW and a total of 20 acquisitions were taken for each spectrum. The spectral resolution was ~ 1μm.

XPS spectroscopy
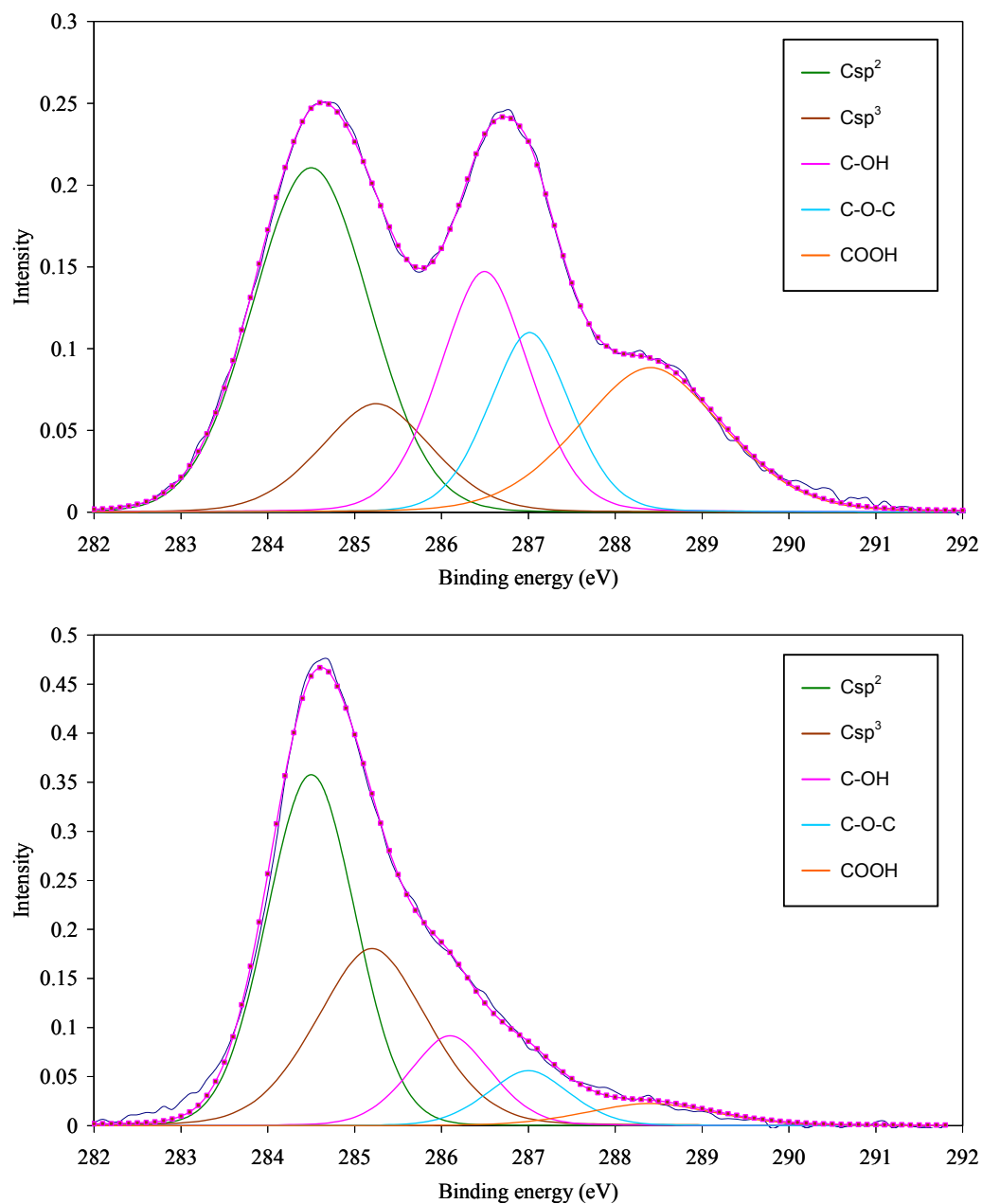
Figure S5. XPS curve fitting of C1s spectra of GO (top) and RGO (bottom). XPS measurements were carried out on a SPECS system operating under 10^{-7} Pa connected to a Mg Kα X-ray source (100 W). XPS C1s peaks were curve-fitted by combining the components and by minimizing the total square-error fit. Curve fitting of the C1s spectra was performed using a Gaussian-Lorentzian peak shape after performing a Shirley background correction.

FTIR spectroscopy

The FTIR spectra were collected on a Nexus Thermo FTIR spectrometer equipped with a DTGS detector (4 cm^{-1} resolution, 32 scans).

S3. Computational details

The calculations were performed at the periodic DFT level by using the VASP program.[2-4] Geometry optimizations were performed until the forces were below 0.015 eV/Å at the periodic DFT level (PW91 functional)[5-6], using the projector-augmented-wave method (PAW) of Blöchl[7] as adapted by Kresse and Joubert[8], and a plane-wave basis set with a kinetic energy cut-off of 400eV. The coordinates of all the atoms in the models were fully optimized. Intermolecular dispersion interactions were corrected using the DFT-D3 method[9] (at the periodic DFT optimized geometries) as implemented by the authors[10]. The CO frequencies were evaluated in a subspace of the Hessian matrix with the degrees of freedom characteristic of the CO molecule and the C atoms belonging to the graphene sheet bonded to C and/or O atoms of the CO molecule. Second derivatives were calculated numerically with ±0.005 and ±0.010 displacements in the case of C and O atoms. Charge population analysis was performed according to Bader´s theory of atoms in molecules (AIM), using the algorithm developed by Henkelman[11-12].

References

(1) I. Horcas; R. Fernandez; J. M. Gomez-Rodriguez; J. Colchero; J. Gomez-Herrero; A. M. Baro *Rev. Sci. Instrum.* 2007, **78**.

(2) G. Kresse; J. Hafner *Phys. Rev. B* 1993, **48**, 13115-13118.

(3) G. Kresse; J. Hafner *Phys. Rev. B* 1994, **49**, 14251-14269.

(4) G. Kresse; J. Furthmuller *Computational Materials Science* 1996, **6**, 15-50.

(5) J. P. Perdew; Y. Wang *Phys. Rev. B* 1992, **45**, 13244-13249.

(6) J. P. Perdew; J. A. Chevary; S. H. Vosko; K. A. Jackson; M. R. Pederson; D. J. Singh; C. Fiolhais *Phys. Rev. B* 1992, **46**, 6671-6687.

(7) P. E. Blöchl *Phys. Rev. B* 1994, **50**, 17953-17979.

(8) G. Kresse; D. Joubert *Phys. Rev. B* 1999, **59**, 1758-1775.

(9) S. Grimme; J. Antony; S. Ehrlich; H. Krieg *The Journal of Chemical Physics* 2010, **132**, 154104.

(10) S. Stankovich; R. D. Piner; X. Q. Chen; N. Q. Wu; S. T. Nguyen; R. S. Ruoff *J. Mater. Chem.* 2006, **16**, 155-158.

(11) G. Henkelman; A. Arnaldsson; H. Jonsson *Computational Materials Science* 2006, **36**, 354-360.

(12) E. Sanville; S. Kenny; R. Smith; G. Henkelman *J. Comput. Chem.* 2007, **28**, 899-908.